Am J Cancer Res 2023;13(3):950-963
www.ajcr.us /ISSN:2156-6976/ajcr0148821

Original Article

Prognostic value of tumor immune microenvironment factors in patients with stage I lung adenocarcinoma

Qianqian Xue[1,2,3], Yue Wang[1,2,3], Qiang Zheng[1,2,3], Lijun Chen[1,2,3], Yicong Lin[1,2,3], Yan Jin[1,2,3], Xuxia Shen[1,2,3], Yuan Li[1,2,3]

[1]Department of Pathology, Fudan University Shanghai Cancer Center, Shanghai, China; [2]Department of Oncology, Shanghai Medical College, Fudan University, Shanghai, China; [3]Institute of Thoracic Oncology, Fudan University, Shanghai, China

Received December 28, 2022; Accepted February 11, 2023; Epub March 15, 2023; Published March 30, 2023

Abstract: Survival is difficult to predict in patients with resected stage I lung adenocarcinoma (LUAD), but tumor microenvironment (TME) factors appear useful in predicting survival in advanced non-small cell lung cancer. We aimed to identify the TME factors linked to recurrence/metastasis and survival in stage I LUAD patients. We evaluated TME factors in stage I LUAD patients in The Cancer Genome Atlas (TCGA) using the "ESTIMATE" and "MCP-counter" R packages. We characterized infiltrating immune cells in the tumor and stromal regions in 44 stage I LUAD patients at our hospital using immunohistochemical methods combined with the HALO® Image Analysis Platform. In TCGA LUAD patients, the number of neutrophils was higher in patients without recurrence/metastasis than in patients with recurrence/metastasis. For patients with recurrence/metastasis, higher CD8+ T lymphocyte and B lymphocyte infiltration levels were associated with better overall survival (OS), and myeloid dendritic cell (DC) infiltration was associated with better disease-free survival (DFS). In stage I LUAD patients at our hospital, CD4+ T cells, CD8+ T cells, CD14+ monocytic lineage cells, CD16+ NK cells, and CD19+ B lymphocytes were more highly expressed in stromal regions than in tumor regions. Moreover, high intratumoral CD11c+ myeloid DC and CD68+ macrophage levels were associated with recurrence/metastasis. Within tumor regions, higher CD11c+ myeloid DC and CD68+ macrophage levels were associated with shorter DFS; within stromal regions, higher CD68+ macrophage levels were associated with shorter DFS. Multivariate analysis revealed that the presence of intravascular carcinoma embolus, higher intratumoral CD11c+ myeloid DC levels, and high stromal CD68+ macrophage and CD4+ T-cell levels were independently linked to recurrence/metastasis in stage I LUAD patients. This study using 2 datasets shows that key players in the TME are associated with recurrence/metastasis in stage I LUAD patients. Higher intratumoral CD11c+ myeloid DC, stromal CD68+ macrophage and stromal CD4+ T-cell levels are independent prognostic factors for DFS in these patients.

Keywords: Stage I lung adenocarcinoma, recurrence, tumor microenvironment, immunohistochemistry, HALO

Introduction

Lung cancer is one of the most common tumors worldwide. According to the International Agency for Research on Cancer (IARC), in 2020, lung cancer had a high incidence, accounting for 11.4% of new cancer cases, and had a poor prognosis, accounting for 18% of cancer deaths [1]. With medical advances, the survival rates of non-small-cell lung cancer (NSCLC) patients have improved over the past 30 years, but the 5-year relative survival rates are still very low [2]. Adenocarcinoma, the most common type of NSCLC, accounts for approximately 40-50% of cases [3]. Surgical resection is preferred for NSCLC patients with stage I-II disease, and appropriate adjuvant therapy after surgery can reduce the probability of distant metastases and improve the 5-year survival rate of patients [4, 5]. With the rapid development of emerging technology platforms (e.g., second-generation sequencing and other genomics) and molecular targeted drugs, an increasing number of lung cancer patients with specific driver genetic alterations have benefited from molecular targeted therapies [4, 5]. Approximately 69% of advanced NSCLC patients have a potential molecular target for treatment [6]. Epidermal

growth factor receptor (EGFR)-tyrosine kinase inhibitors (TKIs) are a common example of targeted treatment, and although targeted therapies have improved survival in patients with metastases, the efficacy in most patients is ultimately limited by the emergence of drug resistance [4]. Unfortunately, although multimodal strategies have been employed in patients with advanced disease to eliminate cancer cells as much as possible, the long-term survival of these patients is still unsatisfactory. Therefore, the top priorities in curing cancer are early detection and timely and adequate treatment [7]. New biomarkers of tumor progression need to be identified, and new therapeutic strategies need to be explored.

In the past decade, it has been well confirmed that the tumor microenvironment (TME) plays an irreplaceable role in the initial onset, growth, progression and invasive metastasis of tumors [8, 9]. Thus, the TME is also considered an environment rich in targets for novel anticancer agents [10]. Many NSCLC patients have benefited from immunotherapy represented by immune checkpoint inhibitors (ICIs). Lung adenocarcinoma (LUAD) has significant cellular and genetic heterogeneity that is present not only in tumor epithelial cells but also in all components of the TME [11]. Therefore, different factors of the TME can indicate disease stage, treatment response and clinical prognosis [12]. As a current research hotspot, the exploration of TME factors as predictive, diagnostic or prognostic biomarkers has also made considerable advances. For example, high levels of FoxP3 (+) T regulatory cells (Tregs) within the TME usually suggest poor clinical outcomes in various cancer patients and correlate with resistance to immunotherapy [13]. Our understanding of the mechanisms by which the TME promotes cancer development is growing. Technological advances such as real-time imaging, fluorescence multiplex immunohistochemistry (mIHC), and transposed convolution algorithm analysis based on large amounts of gene expression data have led to better descriptions of the TME and further promoted the development of anticancer therapies targeting the TME.

Our group found recurrence or distant metastases in a small proportion of early-stage LUAD patients within 1-3 years, with a poor clinical outcome. Accordingly, we aimed to explore the correlation between TME factors and the prognosis of stage I LUAD patients by assessing immune cell profiles using two different methods, namely, bioinformatics and immunohistochemistry (IHC) combined with the HALO® Image Analysis Platform, to identify new biomarkers indicating early recurrence or metastasis and provide new therapeutic targets for early-stage LUAD patients with recurrence/metastasis.

Methods

Study patients

1) The Cancer Genome Atlas (TCGA) database cohort: We downloaded complete RNA sequencing (RNA-seq) data and clinical data of all LUAD patients from the TCGA database (https://tcga-data.nci.nih.gov/tcga/) in September 2020. The raw RNA-seq data were in HTSeq-Counts format. After matching the RNA-seq data with clinical data, we excluded patients with an overall survival (OS) time less than or equal to 60 days and then screened 55 stage I LUAD patients with recurrence/metastasis and 157 stage I LUAD patients without recurrence/metastasis.

2) The Fudan University Shanghai Cancer Center cohort: We randomly selected 22 stage I LUAD patients who developed recurrence/metastasis during the follow-up period and 22 stage I LUAD patients without recurrence/metastasis from patients admitted to the Fudan University Shanghai Cancer Center from September 2016 to May 2018. All enrolled patients were diagnosed with stage I LUAD by histopathological examination according to the 8th edition of the TNM classification. Recurrence/metastasis was confirmed by imaging or histopathological examination for all relevant patients. We collected the clinicopathological data and available formalin-fixed paraffin-embedded (FFPE) specimens for IHC staining of the 44 patients. The clinicopathological characteristics recorded included sex, age, smoking history, tumor size, IASLC grade, intravascular carcinoma embolus, pleural infiltration, and EGFR mutation status. FFPE specimens, hematoxylin-eosin (HE) sections, and pan-cytokeratin (pan-CK) staining sections of all patients were provided by the Department of Pathology, Fudan University Shanghai Cancer Center. All enrolled patients signed informed consent forms at the time of admission. The study was

approved by the Ethics Committee of Fudan University Shanghai Cancer Center.

TME evaluation by bioinformatics analysis

1) R Package "ESTIMATE": We used the "ESTIMATE" package [14] in R (4.0.5) [15] to calculate the immune scores of stage I LUAD patients with recurrence/metastasis and without recurrence/metastasis in the TCGA database. The "ESTIMATE" package is based on the single-sample gene set enrichment analysis (ssGSEA) algorithm, which predicts the number of stromal cells and infiltrating immune cells in tumor tissues using transcriptome expression data and thereby generates three scores: stromal score, immune score, and estimate score (predicting the tumor purity) [14]. That is, the more stromal cells and infiltrating immune cells there are, the higher the stromal score and immune score, respectively; the higher the estimate score, which is the sum of the stromal and immune scores, the lower the tumor purity is.

2) R Package "MCP-counter": TME factors of stage I LUAD patients in the TCGA database were assessed in R (4.0.5) by the "Microenvironment Cell Populations-counter (MCP-counter)" package [16]. The MCP-counter method robustly quantifies the abundances of multiple types of immune cells, including CD3+ T cells, CD8+ T cells, cytotoxic lymphocytes, B lymphocytes, myeloid dendritic cells (DCs), natural killer cells (NK cells), neutrophils, monocytic lineage cells, and stromal cells, including endothelial cells and fibroblasts, in the TME based on transcriptome expression data and calculates abundance scores independently for each sample; as such, these scores can be compared directly to assess the abundance of the corresponding cell types across samples within a cohort [16].

IHC staining

The FFPE tumor tissue of each patient was sectioned into 2 μm serial sections for IHC. The serial sections were stained for IHC markers in the following sequence: CD8, CD4, FoxP3, CD11c, CD19, CD68, CD16, CD14, HE, and pan-CK. CD4 and FoxP3 were stained via double immunofluorescence. HE and pan-CK staining were performed by the Department of Pathology, Fudan University Shanghai Cancer Center.

The sections were dewaxed in xylene and hydrated in a graded ethanol series. Subsequently, the sections were pretreated with the appropriate buffer in an autoclave at 115°C for 5 min and then at 100°C for 10 min. Ethylenediaminetetraacetic acid (EDTA) buffer (pH = 9.0) was suitable for CD8, CD14, CD19, CD4 and FoxP3 staining, while sodium citrate buffer (pH = 6.0) was suitable for CD11c, CD16 and CD68 staining.

1) Diaminobenzidine (DAB) color development: The sections were incubated in 3% hydrogen peroxide (H_2O_2) for 10 min to block endogenous peroxidase and then incubated with the corresponding diluted primary antibodies at 4°C overnight. The primary antibodies were anti-CD8α (D8A8Y) rabbit monoclonal antibody (mAb) (#85336, CST, dilution 1:200), anti-CD11c (D3V1E) XP® rabbit mAb (#45581, CST, dilution 1:400), anti-CD14 (D7A2T) rabbit mAb (#75181, CST, dilution 1:600), anti-CD16 (D1-N9L) rabbit mAb (#24326, CST, dilution 1:400), anti-CD19 (intracellular domain) (D4V4B) XP® rabbit mAb (#90176, CST, dilution 1:1000) and anti-CD68 (D4B9C) XP® rabbit mAb (#76437, CST, dilution 1:600). After the sections were incubated with the secondary antibody for 1 hour at room temperature, DAB was used as the chromogen. Finally, the sections were counterstained with hematoxylin and mounted.

2) Double immunofluorescence labeling method: The sections were incubated with the diluted mixed primary antibodies at 4°C overnight and then incubated with the diluted mixed secondary antibodies at room temperature in the dark for 2 hours. The primary antibodies were anti-CD4 antibody [EPR6855] (ab133616, Abcam, dilution 1:100) and anti-FOXP3 antibody [236A/E7] (ab20034, Abcam, dilution 1:100) mixed at a 1:1 ratio. The secondary antibodies were Alexa Fluor® 488 Donkey Anti-Rabbit IgG (Jackson, dilution 1:200) and Alexa Fluor® 594 Donkey Anti-Rat IgG (Jackson, dilution 1:200) mixed at a 1:1 ratio. Finally, nuclei were stained blue with DAPI, and sections were mounted with fluorescence mounting medium.

All sections were scanned as images by an automatic digital slide scanner (PANNORAMIC

MIDI II) and quantitatively analyzed by the HALO® Image Analysis Platform.

Statistical analysis

For the TCGA database cohort, comparisons of immune scores and the abundances of each cell type were performed with the Wilcoxon test in R (4.0.5). For the Fudan University Shanghai Cancer Center cohort, the analysis of clinicopathological characteristics was accomplished by Fisher's exact test, and the differences in immune cell infiltration were evaluated by the Wilcoxon test in Stata16. Survival curves were estimated using the Kaplan-Meier method. Univariate and multivariate Cox regression analyses were performed with the package "survival" in R (4.0.5). A *P* value < 0.05 was considered statistically significant.

Results

Evaluation of TME factors and their correlation with prognosis in the TCGA database cohort

For the 55 stage I LUAD patients with recurrence/metastasis and 157 stage I LUAD patients without recurrence/metastasis from the TCGA database, we calculated immune scores using the R package "ESTIMATE". The results showed that patients without recurrence/metastasis had slightly higher stromal scores, immune scores and estimate scores than patients with recurrence/metastasis; that is, patients without recurrence/metastasis had more stromal cells and immune cells and lower tumor purity; however, the differences were not statistically significant (P > 0.05, **Figure 1A**).

Next, we evaluated the TME of these patients using the MCP-counter method. We compared the TME of patients with and without recurrence/metastasis, and the findings are shown in **Figure 1B**. The number of neutrophils was significantly reduced in patients with recurrence/metastasis compared with those without recurrence/metastasis (P < 0.01).

Finally, we analyzed the TME combined with patient survival data. In patients without recurrence/metastasis, a high abundance of fibroblasts was somewhat associated with reduced OS (P = 0.057, **Figure 1C**), whereas in patients with recurrence/metastasis, a high abundance of CD8+ T cells (P < 0.05, **Figure 1D**) and B lymphocytes (P < 0.05, **Figure 1E**) was associated with increased OS, and a high abundance of myeloid DCs was associated with longer disease-free survival (DFS) (P < 0.01, **Figure 1F**).

Clinicopathological characteristics of the Fudan University Shanghai Cancer Center cohort

A total of 44 patients with stage I LUAD were included in this study, 22 of whom presented with recurrence/metastasis and 22 of whom did not have recurrence/metastasis. The clinicopathological characteristics of all patients are listed in **Table 1**. We found that there were no significant differences in age, sex, smoking history, T stage, pleural infiltration or EGFR mutation status between the patients with and without recurrence/metastasis. However, patients with recurrence/metastasis were more likely to have IASLC grade 2 or 3 disease, whereas patients without recurrence/metastasis were more likely to have IASLC grade 1 or 2 disease (P < 0.05). In addition, intravascular carcinoma embolus was found in 7 (31.8%) of the patients with recurrence/metastasis, whereas no intravascular carcinoma embolus was found in patients without recurrence/metastasis, with a statistically significant difference (P < 0.01).

HALO analysis based on IHC

In this study, we evaluated markers of immune cells in the tumor immune microenvironment (TIME) of each patient by using IHC staining of serial sections: CD8 (to estimate CD8+ T-cell levels), CD4 and FoxP3 (to estimate Treg levels), CD11c (to estimate myeloid DC levels), CD19 (to estimate B lymphocyte levels), CD68 (to estimate macrophage levels), CD16 (to estimate NK cell levels), and CD14 (to estimate monocytic lineage cell levels). The IHC staining results of a representative patient are shown in **Figure 2**.

After IHC staining was completed and the slides were scanned, we quantified the infiltration of various types of immune cells in the patients' tumor tissues using the HALO® Image Analysis Platform (Indica Labs, USA). First, on the HE staining images, we circled the core region of the tumor for analysis and excluded the region of normal lung tissue (**Figure 3A**). Subsequently, we moved the circled tumor core region to the

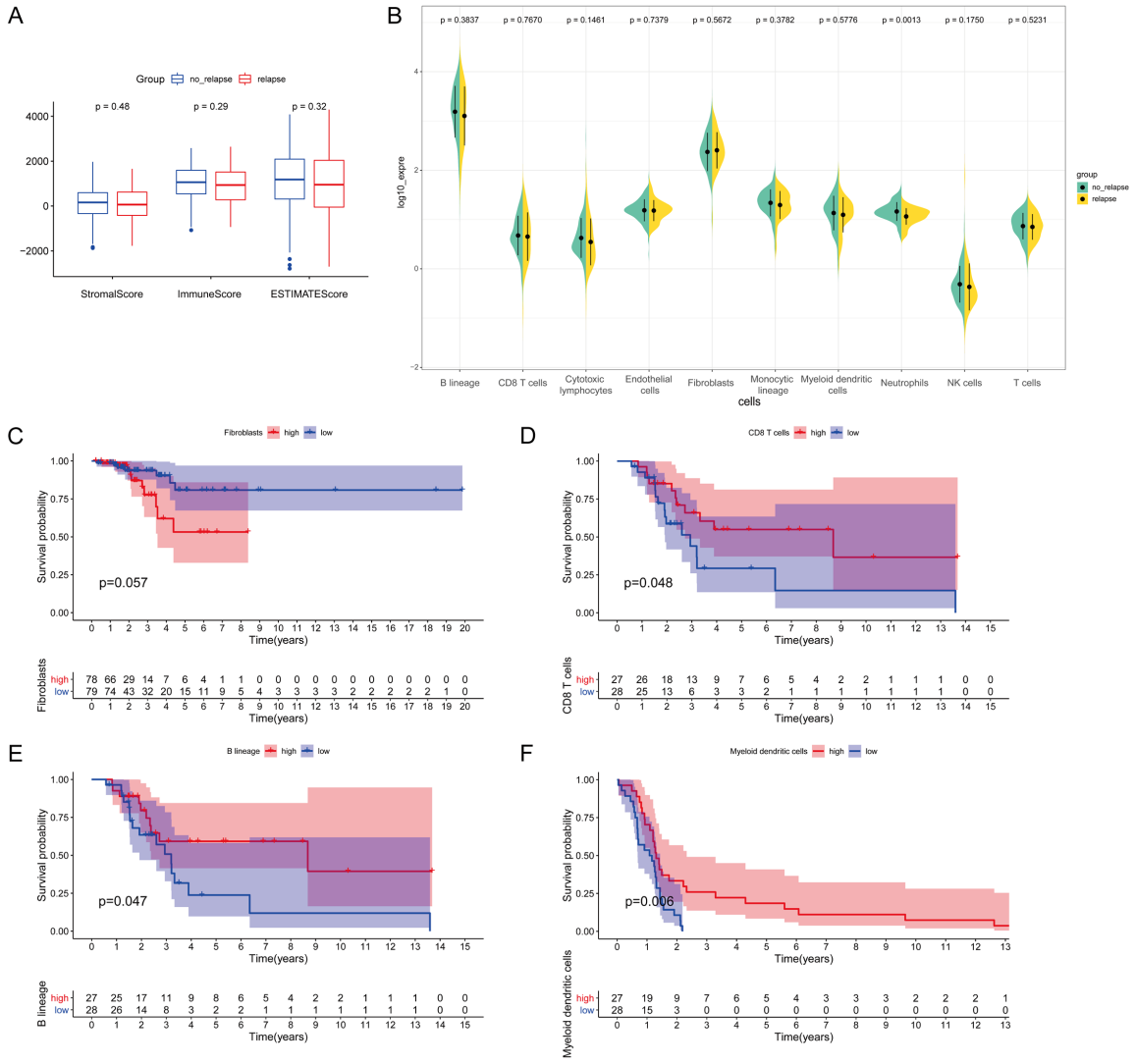

Figure 1. (A, B) Comparison of immune scores (A) and TME factors (B) between stage I LUAD patients with and without recurrence/metastasis from the TCGA database. (C) Kaplan-Meier curves showing the OS of stage I LUAD patients without recurrence/metastasis according to fibroblast abundance. (D) Kaplan-Meier curves showing the OS of stage I LUAD patients with recurrence/metastasis according to CD8+ T-cell abundance. (E) Kaplan-Meier curves showing the OS of stage I LUAD patients with recurrence/metastasis according to B-lymphocyte abundance. (F) Kaplan-Meier curves showing the DFS of stage I LUAD patients with recurrence/metastasis according to myeloid DC abundance.

pan-CK staining image and classified the tumor core region according to the pan-CK staining results. As shown in **Figure 3B**, red areas were pan-CK-positive regions, representing tumor cells within the tumor core region, and green areas were pan-CK-negative regions, representing stromal cells within the tumor core region. Finally, we randomly circled five regions within the tumor cell and stromal cell areas (**Figure 3C**) and moved these circular regions to the corresponding positions on the remaining IHC staining images. We counted the numbers of 1+, 2+, and 3+ positive cells for all indicators within the circular regions (**Figure 3D**, **3E**), calculated the relevant percentages, and obtained the percentage of total positive cells and the histochemistry score (H-score) for each immune cell type within the tumor cell and stromal cell areas for each patient (the H-score could not be calculated for double-positive cells). The

Table 1. Clinicopathological characteristics of stage I LUAD patients from the Fudan University Shanghai Cancer Center

	With recurrence/metastasis (n = 22)		Without recurrence/metastasis (n = 22)		*P* value
	No.	%	No.	%	
Age (years)					0.537
≤ 60	12	54.5	15	68.2	
> 60	10	45.5	7	31.8	
Sex					1.000
Male	11	50.0	11	50.0	
Female	11	50.0	11	50.0	
Smoking status					1.000
Yes	9	40.9	9	40.9	
Never	13	59.1	13	59.1	
T stage					1.000
T1b	9	40.9	9	40.9	
T1c	10	45.5	10	45.5	
T2a	3	13.6	3	13.6	
IASLC grade					0.028
Grade 1	0	0	4	18.2	
Grade 2	10	45.5	13	59.1	
Grade 3	12	54.5	5	22.7	
Intravascular carcinoma embolus					0.009
Present	7	31.8	0	0	
Absent	15	68.2	22	100.0	
Pleural infiltration					0.340
Present	9	40.9	6	27.3	
Absent	13	59.1	16	72.7	
EGFR mutation status					0.177
Mutant	13	59.1	17	77.3	
Wild-type	5	22.7	1	4.5	
NA	4	18.2	4	18.2	

H-score was calculated as follows: H-score = [1× (%1+ cells) + 2× (%2+ cells) + 3× (%3+ cells)].

Evaluation of TIME factors and their correlation with prognosis in the Fudan University Shanghai Cancer Center cohort

We selected two indicators, the percentage of total positive cells and the H-score, to assess the immune cell profiles of the Fudan University Shanghai Cancer Center cohort. First, we analyzed the differences in immune cell infiltration within the tumor and stromal regions, which revealed that compared with the tumor regions, the stromal regions showed higher percentages of positive-staining cells and H-scores for CD8+ T cells, CD14+ monocytic lineage cells, CD16+ NK cells, CD19+ B lymphocytes, and CD4+ T cells (**Figure 4A**). In contrast, in patients with recurrence/metastasis, the percentages of positive-staining cells and H-scores for only CD19+ B lymphocytes and CD4+ T cells were higher within the stromal regions (**Figure 4B**); in patients without recurrence/metastasis, the percentages of positive-staining cells and H-scores for only CD8+ T cells, CD14+ monocytic lineage cells, CD19+ B lymphocytes, and CD4+ T cells were higher within the stromal regions (**Figure 4C**).

Subsequently, we further analyzed the differences in immune cell infiltration between patients with and without recurrence/metastasis. Compared with patients without recurrence/metastasis, patients with recurrence/

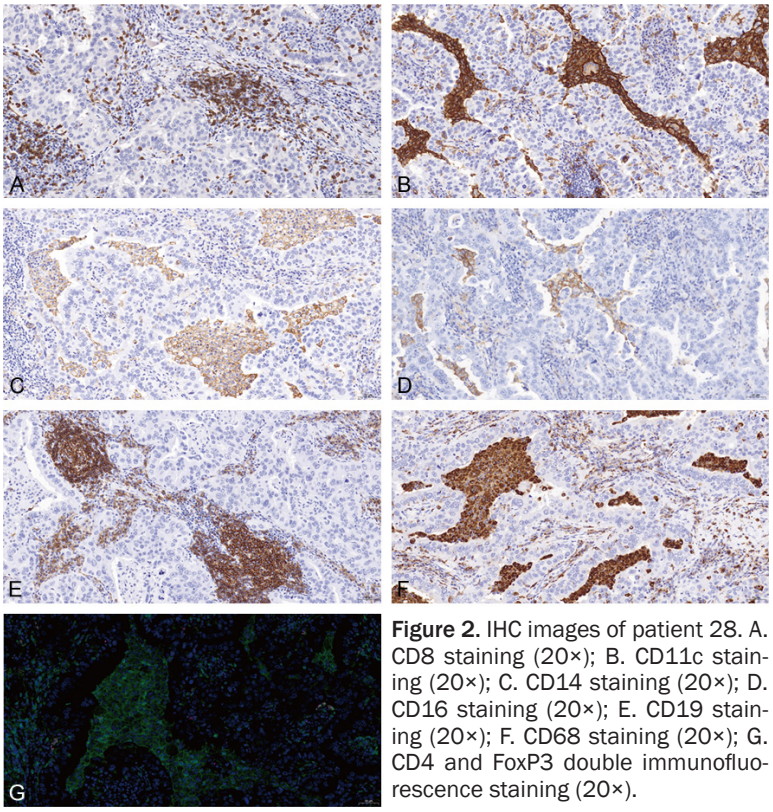

Figure 2. IHC images of patient 28. A. CD8 staining (20×); B. CD11c staining (20×); C. CD14 staining (20×); D. CD16 staining (20×); E. CD19 staining (20×); F. CD68 staining (20×); G. CD4 and FoxP3 double immunofluorescence staining (20×).

metastasis had higher percentages of positive-staining cells and H-scores for intratumoral CD11c+ myeloid DCs and intratumoral CD68+ macrophages (**Figure 5A**), while no significant difference was observed within the stromal regions (**Figure 5B**). Additionally, in patients without recurrence/metastasis, the difference between stromal CD11c+ myeloid DC and intratumoral CD11c+ myeloid DC expression was much higher than that in patients with recurrence/metastasis (**Figure 5C**).

Finally, according to the percentages of positive-staining cells and the H-scores of each immune cell type, we divided the patients into high- and low-infiltration groups and further analyzed the survival data. Survival analysis demonstrated that higher percentages of intratumoral CD11c+ myeloid DCs and a higher H-score for intratumoral CD11c+ myeloid DCs were associated with shorter DFS (**Figure 6A**), and a higher percentage of intratumoral CD68+ macrophages was associated with shorter DFS (**Figure 6B**). Additionally, a higher percentage of stromal CD68+ macrophages was likewise associated with shorter DFS (**Figure 6C**), while a higher percentage of stromal CD4+ T cells was somewhat associated with shorter DFS, although the difference was not statistically significant (P = 0.093, **Figure 6D**).

Independent prognostic predictors in the Fudan University Shanghai Cancer Center cohort

Univariate Cox regression analysis of clinicopathological characteristics and positive-staining cell percentages for each immune cell type within the tumor and stromal regions was conducted, and the results are shown in **Table 2**. The variables with a *P* value < 0.1 were further included in the multivariate Cox regression analysis, and the results indicated that the presence of intravascular carcinoma embolus and high levels of intratumoral CD11c+ myeloid DCs, stromal CD68+ macrophages and stromal CD4+ T-cell expression were independent risk factors associated with recurrence/metastasis in stage I LUAD patients (**Table 3**).

Discussion

It has been widely demonstrated that the TME plays a crucial role in the initial onset, growth, progression and treatment response of tumors. In this study, to investigate the impact of the TME on recurrence/metastasis in early-stage LUAD patients, we used two methods, bioinformatics and IHC combined with the HALO® Image Analysis Platform, to assess the TME of stage I LUAD patients from the TCGA database and Fudan University Shanghai Cancer Center.

For stage I LUAD patients from the TCGA database, we used different algorithms to assess the TME based on transcriptomic data. In patients with definite recurrence/metastasis, high infiltration of CD8+ T cells and B lymphocytes suggested better OS, and high infiltration of myeloid DCs suggested better DFS. In addition, the patients without recurrence/metastasis had a higher abundance of neutrophils than

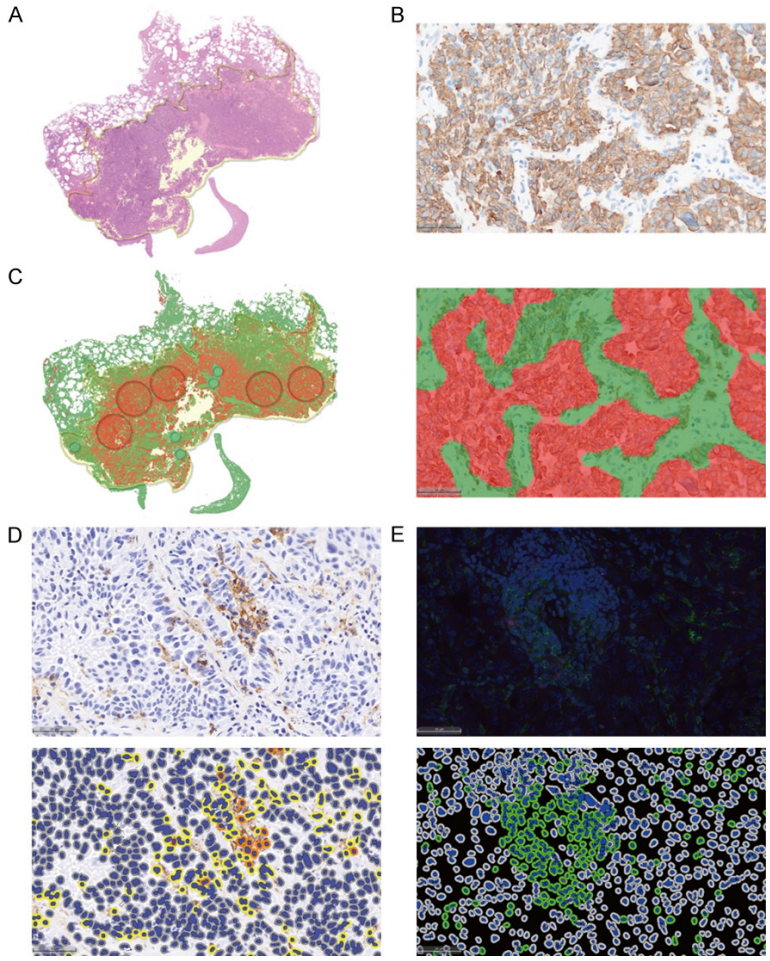

Figure 3. Schematic diagram of the HALO analysis process. A. The yellow circle is the core region of the tumor. B. Pan-CK staining (top). The red regions contain tumor cells, and the green regions contain stromal cells (bottom). C. Core region of the tumor (yellow circle); tumor cells (red circle); stromal cells (green circle). D. Quantitative analysis of images stained by the DAB method. E. Quantitative analysis of images stained by the double immunofluorescence labeling method.

those with recurrence/metastasis. For the 44 stage I LUAD patients from the Fudan University Shanghai Cancer Center, we used IHC combined with the HALO® Image Analysis Platform to assess the TIME. IHC is widely applied in daily clinical work. In contrast to flow cytometry, which does not provide spatial information, IHC staining utilizes prepared FFPE tissue specimens, which are widely available, and IHC staining can be used to characterize the expression of individual markers and obtain spatial data on the localization of marker expression at a single time point and can be readily performed with a brightfield microscope. Moreover, application of the HALO® Image Analysis Platform can provide more accurate and consistent analysis data than manual interpretation. Based on our findings, CD4+ T cells, CD8+ T cells, CD19+ B lymphocytes, CD16+ NK cells and CD14+ monocytic lineage cells were more frequently located in the stromal regions than in the tumor regions. The number of intratumoral CD11c+ myeloid DCs and intratumoral CD68+ macrophages was higher in patients with recurrence/metastasis than in those without recurrence/metastasis. High levels of intratumoral CD11c+ myeloid DCs, intratumoral CD68+ macrophages and stromal CD68+ macrophages were associated with a shorter DFS. In addition, multivariate Cox regression analysis demonstrated that high infiltration of intratumoral CD11c+ myeloid DCs, stromal CD68+ macrophages and stromal CD4+ T cells was an independent risk factor for recurrence/metastasis in stage I LUAD patients.

CD8+ T cells are related to acquired immunity and perform key cytotoxic roles in the TME. CD8+ cytotoxic T cells induce tumor clearance by producing interferon gamma (IFN-γ), tumor necrosis factor (TNF), and granzyme B, which target and kill tumor cells [17]. Tumor-infiltrating B lymphocytes (TIBs) are also key players in the TME and are present at all stages of lung cancer development [18, 19]. Many studies have demonstrated that NSCLC patients with high infiltration of CD20+ B lymphocytes have a better clinical outcome [20-26], while a few studies have not found a significant association [21, 27-29]. Moreover, in NSCLC patients, follicular B cells and mature DCs have been observed within tertiary lymphoid structures (TLSs), the density of follicular B cells was found to be positively correlated with the density of mature DCs, the density of lysosomal associated membrane protein 3 (LAMP3)-positive mature DCs was found to be positively correlated with the

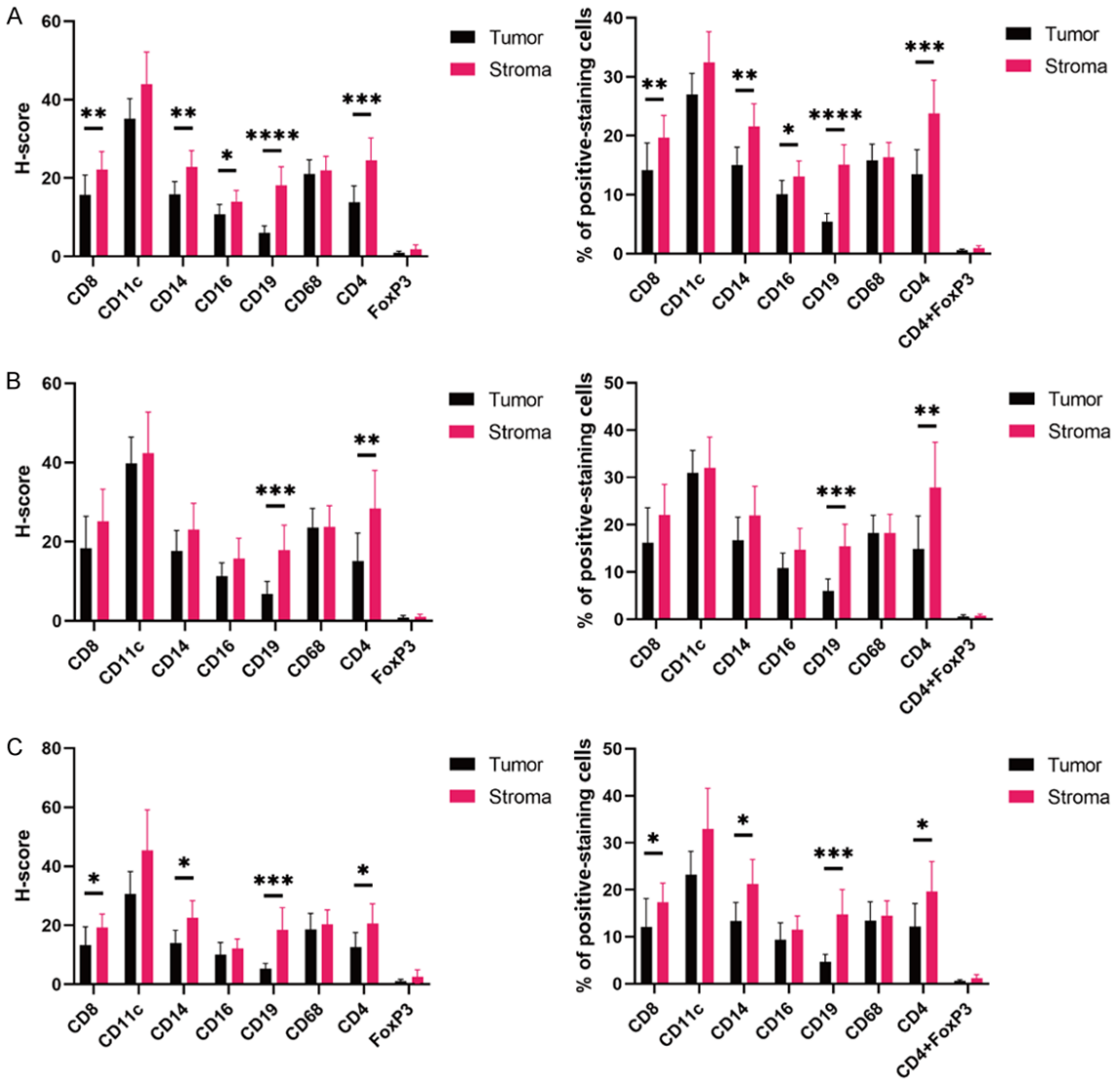

Figure 4. Immune cell infiltration in the Fudan University Shanghai Cancer Center Cohort, with the H-score in the left column and the percentage of total positive cells in the right column. Differences in immune cell infiltration between the tumor regions and stromal regions in all patients (A), patients with recurrence/metastasis (B), and patients without recurrence/metastasis (C). $^{*}P < 0.05$, $^{**}P < 0.01$, $^{***}P < 0.001$, $^{****}P < 0.0001$.

infiltration of cytotoxic T cells, and an increased density of both follicular B cells and mature DCs was found to indicate good clinical outcome [20, 30, 31]. As a class of polymorphonuclear granulocytes, neutrophils were named for their preference to uptake pH-neutral dyes, but they are no longer considered "neutral" in the cancer setting, as they have different phenotypes in each step of cancer development and sometimes have opposing functions [32]. In lung cancer, intratumoral neutrophils seem to play this type of controversial role [33]. As an example, in one study, the density of CD66b+ tumor-associated neutrophils (TANs) was an independent positive prognosticator in squamous carcinoma patients but an independent negative prognosticator in adenocarcinoma patients [34]. In contrast, Liu, X. et al. reported that a high density of neutrophils predicted a poor prognosis in squamous carcinoma patients, while no such correlation was observed in adenocarcinoma patients [35]. Carus, A. et al. concluded that the density of CD66b+ TANs was not directly related to OS or DFS in NSCLC patients [36]. Tumor-associated macrophages (TAMs) include two phenotypes with different

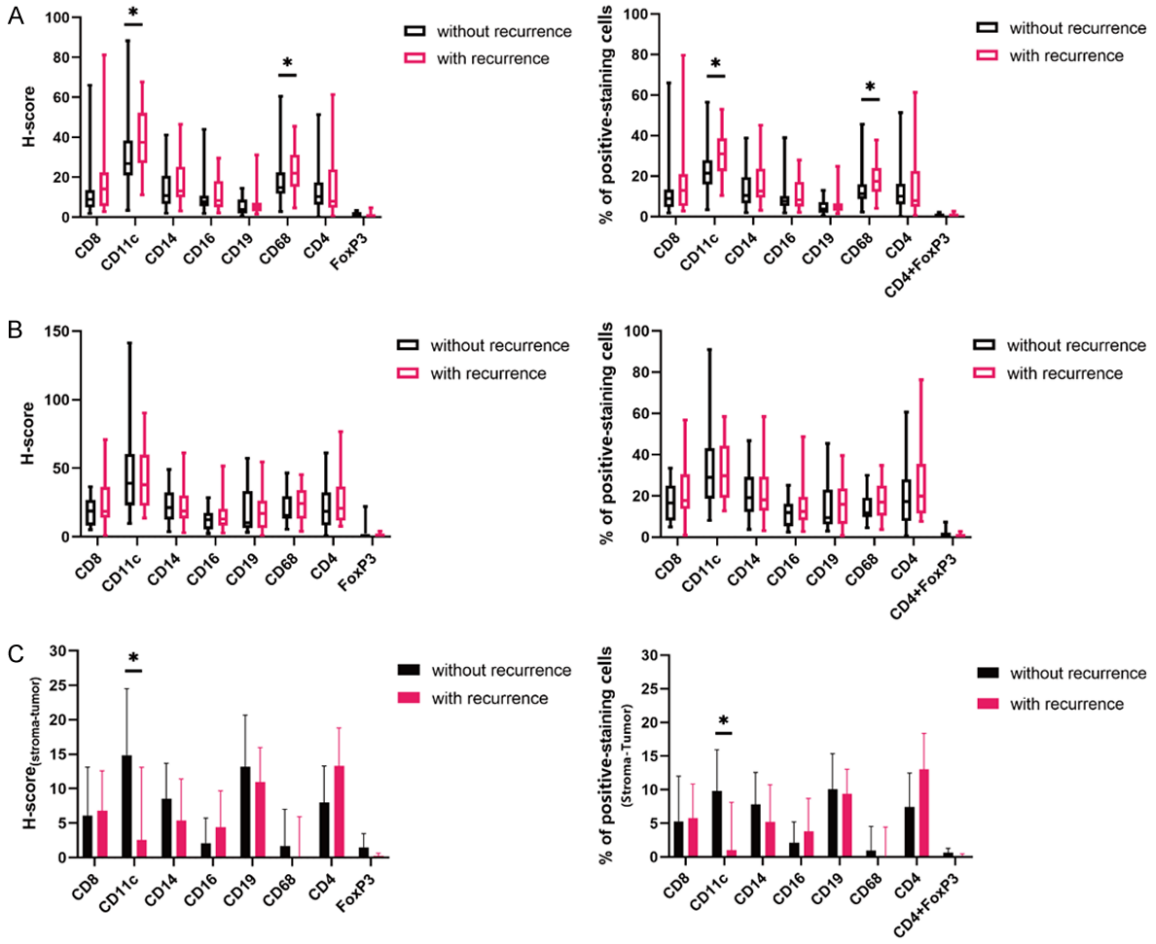

Figure 5. (A, B) Differences in immune cell infiltration between patients with and without recurrence/metastasis within tumor regions (A) and stromal regions (B). (C) Difference in immune cell infiltration between stromal and intratumoral areas in patients with and without recurrence/metastasis. *P < 0.05.

functions, M1 and M2. M1 macrophages suppress tumor development, while M2 macrophages promote tumor development. Extensive interactions exist between TAMs and NSCLC tumor cells. For example, NSCLC tumor cells secrete interleukin-17 (IL-17) and prostaglandin-E2 (PGE2), and IL-17 recruits TAMs, while PGE2 induces M2 macrophage differentiation [37]. Furthermore, TAMs release several molecules, such as vascular endothelial growth factor (VEGF), urokinase-type plasminogen activator (uPA), cyclooxygenase-2 (COX-2) and matrix metalloproteinase-9 (MMP-9), creating a suitable microenvironment for the progression of NSCLC and the invasion of NSCLC tumor cells [38]. The prognostic predictive value of TAMs in NSCLC patients has also been reported. In surgically resected NSCLC patients, an increased density of tumor islet CD68+ macrophages was an independent determinant of a favorable outcome, whereas an increased density of stromal CD68+ macrophages was an independent determinant of reduced survival [39]. CD204+ macrophages in the stroma, probably M2 macrophages, were significantly associated with lymphatic permeation, vessel invasion, and pleural invasion, and suggested a poor prognosis [40]. The opposite conclusion has also been proposed. In the study by Rakaee M et al., using multiplex immunohistochemistry, high infiltration levels of either intratumoral or stromal pan-CD68, HLA-DR+ M1, and CD204+ M2 macrophages were considered independent indicators of good prognosis [41]. Using biopsy specimens from stage IV NSCLC patients, Kawai O et al. reported that patients with more TAMs in cancer nests than in stroma had a significantly better clinical outcome than those

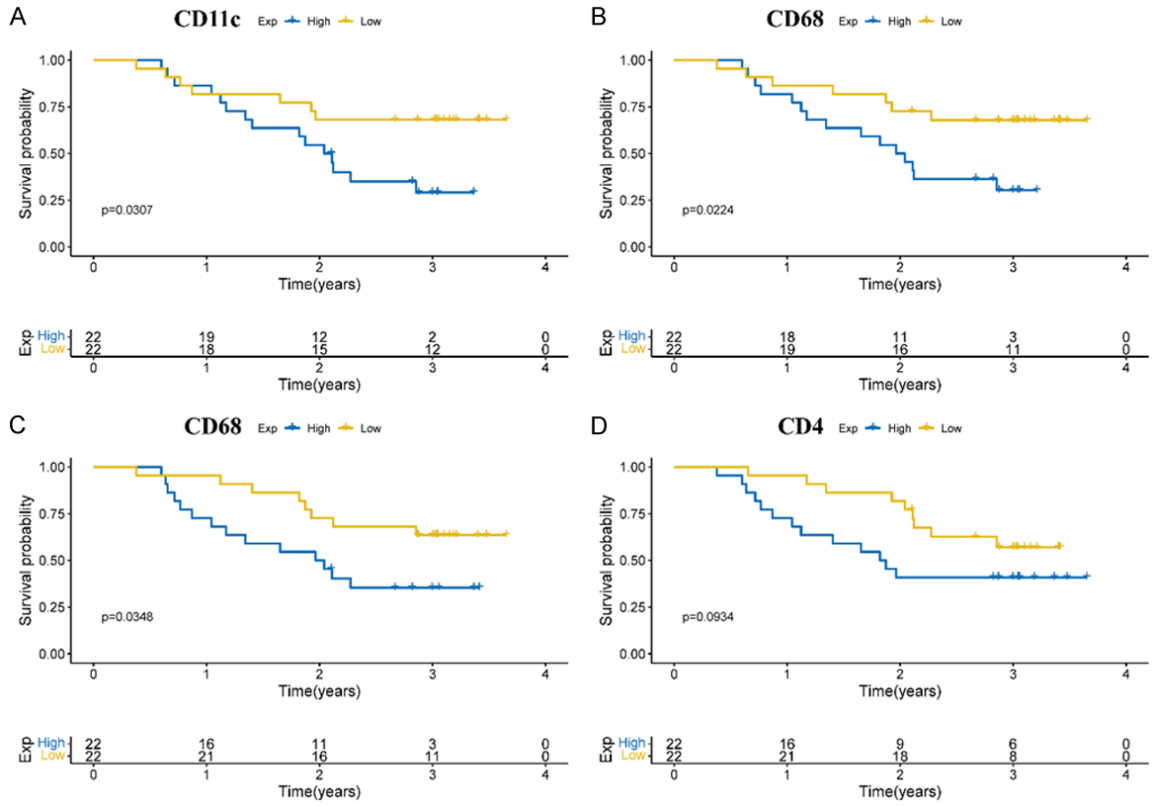

Figure 6. Kaplan-Meier DFS curves of stage I LUAD patients from the Fudan University Shanghai Cancer Center. A. Intratumoral CD11c expression. B. Intratumoral CD68 expression. C. Stromal CD68 expression. D. Stromal CD4 expression.

with more TAMs in stroma than in cancer nests, but this index could not predict chemotherapy response [42].

We reviewed some literature about the clinical impact of TME factors in early-stage LUAD. A study by Kinoshita, F. et al. divided stage IA LUAD patients into four groups (CD8-low/FoxP3-low, CD8-high/FoxP3-low, CD8-low/FoxP3-high and CD8-high/FoxP3-high), and the results demonstrated that the CD8-low/FoxP3-high group was more likely to have an immunosuppressed status, and the CD8-low/FoxP3-high phenotype was an independent risk factor for DFS in stage IA LUAD patients [43]. Similar conclusions have also been reported in other studies. In patients with stage I LUAD, a high density of stromal FoxP3-positive cells indicates shorter DFS, but the ratio of FoxP3-positive to CD3-positive cells was a better predictor of relapse [28]. Positive PD-L1 expression and low intratumoral CD8 expression were identified as independent prognostic factors in stage I NSCLC patients [44].

Immune cells are highly heterogeneous and plastic in function. Most immune cells behave differently depending on their activation status and the surrounding microenvironment. Therefore, the findings of TME-related studies are not always consistent. In our study, two completely different methods were used to assess the immune cell profiles of stage I LUAD patients, and the findings were partly consistent with published studies. Thus, the accuracy of the two methods, bioinformatics analysis based on transcriptomic data and IHC combined with HALO® Image Analysis Platform analysis, in assessing the correlation between TME factors and recurrence/metastasis in stage I LUAD patients needs to be further validated in the future.

Undoubtedly, there are also a few shortcomings in our study. Because our study subjects were stage I LUAD patients and FFPE tissue blocks that have been preserved for extended periods of time often have poor antigenicity, our study cohort was relatively small. In addition, the

Table 2. Univariate Cox regression analysis of DFS based on clinicopathological characteristics and TIME factors

Variable	HR	95% CI	*P* value
Age	1.033	(0.972-1.097)	0.300
Sex	1.103	(0.477-2.550)	0.820
Smoking history	1.059	(0.452-2.480)	0.900
Tumor size	1.015	(0.559-1.845)	0.960
IASLC grade	2.877	(1.341-6.171)	0.007
Intravascular carcinoma embolus	5.317	(2.095-13.490)	0.000
Pleural infiltration	1.533	(0.654-3.597)	0.330
EGFR mutation status	0.270	(0.093-0.783)	0.016
Intratumoral CD8 expression	1.009	(0.987-1.033)	0.420
Intratumoral CD11c expression	1.037	(1.004-1.071)	0.029
Intratumoral CD14 expression	1.018	(0.981-1.058)	0.340
Intratumoral CD16 expression	1.017	(0.969-1.068)	0.490
Intratumoral CD19 expression	1.037	(0.952-1.131)	0.400
Intratumoral CD68 expression	1.035	(0.997-1.075)	0.071
Intratumoral CD4 expression	1.010	(0.981-1.041)	0.490
Intratumoral CD4+FoxP3 expression	0.937	(0.527-1.666)	0.820
Stromal CD8 expression	1.028	(0.995-1.062)	0.092
Stromal CD11c expression	1.001	(0.978-1.024)	0.960
Stromal CD14 expression	1.004	(0.973-1.036)	0.810
Stromal CD16 expression	1.020	(0.981-1.060)	0.310
Stromal CD19 expression	1.007	(0.972-1.044)	0.700
Stromal CD68 expression	1.046	(0.997-1.097)	0.068
Stromal CD4 expression	1.020	(1.000-1.040)	0.055
Stromal CD4+FoxP3 expression	0.831	(0.560-1.233)	0.360

Table 3. Multivariate Cox regression analyses of DFS in patients with stage I LUAD

Variable	HR	95% CI	*P* value
IASLC grade	1.694	(0.533-5.385)	0.372
Intravascular carcinoma embolus	6.857	(1.462-32.151)	0.015
EGFR mutation status	0.225	(0.046-1.103)	0.066
Intratumoral CD11c expression	1.081	(1.012-1.155)	0.021
Intratumoral CD68 expression	0.952	(0.874-1.036)	0.250
Stromal CD8 expression	0.971	(0.926-1.018)	0.225
Stromal CD68 expression	1.111	(1.016-1.214)	0.021
Stromal CD4 expression	1.033	(1.002-1.065)	0.038

chromogenic IHC (cIHC) staining we used provided relatively limited information compared to the emerging fluorescent mIHC. Fluorescent mIHC allows for the simultaneous detection of multiple markers on a single section to gather maximal data and provides researchers with a comprehensive view of the coexpression and spatial organization of multiple markers. There are also a number of well-established commercial fluorescent mIHC panels for TME assessment. In the future, we plan to apply fluorescent mIHC combined with the HALO® Image Analysis Platform to analyze the spatial organization of immune cells for a more in-depth study of the TME in early-stage LUAD patients.

Conclusions

We used two different methods to comprehensively assess the TME of two stage I LUAD groups, evaluated the correlation between TME factors and recurrence/metastasis, and provided valuable predictors of the prognosis of early-stage LUAD patients.

Acknowledgements

This research was funded by the National Natural Science Foundation of China, grant number 81972171; the CSCO-PILOT Cancer Research Foundation, grant number Y-2019AZMS-0492; and the National Key Research and Development Program of China, grant number 2021YFF1201001.

Disclosure of conflict of interest

None.

Address correspondence to: Yuan Li, Department of Pathology, Fudan University Shanghai Cancer Center, Shanghai, China. Tel: +86-21-6417-5590; E-mail: whliyuan@hotmail.com

References

[1] Sung H, Ferlay J, Siegel RL, Laversanne M, Soerjomataram I, Jemal A and Bray F. Global cancer statistics 2020: GLOBOCAN estimates of incidence and mortality worldwide for 36 cancers in 185 countries. CA Cancer J Clin 2021; 71: 209-249.

[2] Wang S, Sun T, Sun H, Li X, Li J, Zheng X, Mallampati S, Sun H, Zhou X, Zhou C, Zhang H, Cheng Z and Ma H. Survival improvement in patients with non-small cell lung cancer between 1983 and 2012: analysis of the surveil-

lance, epidemiology, and end results database. Tumour Biol 2017; 39: 10104283-17691677.
[3] Osmani L, Askin F, Gabrielson E and Li QK. Current WHO guidelines and the critical role of immunohistochemical markers in the subclassification of non-small cell lung carcinoma (NSCLC): moving from targeted therapy to immunotherapy. Semin Cancer Biol 2018; 52: 103-109.
[4] Duma N, Santana-Davila R and Molina JR. Non-small cell lung cancer: epidemiology, screening, diagnosis, and treatment. Mayo Clin Proc 2019; 94: 1623-1640.
[5] Miller KD, Nogueira L, Mariotto AB, Rowland JH, Yabroff KR, Alfano CM, Jemal A, Kramer JL and Siegel RL. Cancer treatment and survivorship statistics, 2019. CA Cancer J Clin 2019; 69: 363-385.
[6] Hirsch FR, Scagliotti GV, Mulshine JL, Kwon R, Curran WJ Jr, Wu YL and Paz-Ares L. Lung cancer: current therapies and new targeted treatments. Lancet 2017; 389: 299-311.
[7] Wang S, Liu Y, Feng Y, Zhang J, Swinnen J, Li Y and Ni Y. A review on curability of cancers: more efforts for novel therapeutic options are needed. Cancers (Basel) 2019; 11: 1782.
[8] Quail DF and Joyce JA. Microenvironmental regulation of tumor progression and metastasis. Nat Med 2013; 19: 1423-1437.
[9] Hinshaw DC and Shevde LA. The tumor microenvironment innately modulates cancer progression. Cancer Res 2019; 79: 4557-4566.
[10] Bejarano L, Jordao MJC and Joyce JA. Therapeutic targeting of the tumor microenvironment. Cancer Discov 2021; 11: 933-959.
[11] Chen Z, Fillmore CM, Hammerman PS, Kim CF and Wong KK. Non-small-cell lung cancers: a heterogeneous set of diseases. Nat Rev Cancer 2014; 14: 535-546.
[12] Altorki NK, Markowitz GJ, Gao D, Port JL, Saxena A, Stiles B, McGraw T and Mittal V. The lung microenvironment: an important regulator of tumour growth and metastasis. Nat Rev Cancer 2019; 19: 9-31.
[13] Saleh R and Elkord E. FoxP3$^+$ T regulatory cells in cancer: prognostic biomarkers and therapeutic targets. Cancer Lett 2020; 490: 174-185.
[14] Yoshihara K, Shahmoradgoli M, Martinez E, Vegesna R, Kim H, Torres-Garcia W, Trevino V, Shen H, Laird PW, Levine DA, Carter SL, Getz G, Stemke-Hale K, Mills GB and Verhaak RG. Inferring tumour purity and stromal and immune cell admixture from expression data. Nat Commun 2013; 4: 2612.
[15] R Core Team (2020). R: a language and environment for statistical computing. R Foundation for Statistical Computing, Vienna, Austria. URL https://www.R-project.org/.
[16] Becht E, Giraldo NA, Lacroix L, Buttard B, Elarouci N, Petitprez F, Selves J, Laurent-Puig P, Sautes-Fridman C, Fridman WH and de Reynies A. Estimating the population abundance of tissue-infiltrating immune and stromal cell populations using gene expression. Genome Biol 2016; 17: 218.
[17] Dunn GP, Old LJ and Schreiber RD. The three Es of cancer immunoediting. Annu Rev Immunol 2004; 22: 329-360.
[18] Wang SS, Liu W, Ly D, Xu H, Qu L and Zhang L. Tumor-infiltrating B cells: their role and application in anti-tumor immunity in lung cancer. Cell Mol Immunol 2019; 16: 6-18.
[19] Patel AJ, Richter A, Drayson MT and Middleton GW. The role of B lymphocytes in the immunobiology of non-small-cell lung cancer. Cancer Immunol Immunother 2020; 69: 325-342.
[20] Germain C, Gnjatic S, Tamzalit F, Knockaert S, Remark R, Goc J, Lepelley A, Becht E, Katsahian S, Bizouard G, Validire P, Damotte D, Alifano M, Magdeleinat P, Cremer I, Teillaud JL, Fridman WH, Sautes-Fridman C and Dieu-Nosjean MC. Presence of B cells in tertiary lymphoid structures is associated with a protective immunity in patients with lung cancer. Am J Respir Crit Care Med 2014; 189: 832-844.
[21] Schalper KA, Brown J, Carvajal-Hausdorf D, McLaughlin J, Velcheti V, Syrigos KN, Herbst RS and Rimm DL. Objective measurement and clinical significance of TILs in non-small cell lung cancer. J Natl Cancer Inst 2015; 107: dju435.
[22] Kinoshita T, Muramatsu R, Fujita T, Nagumo H, Sakurai T, Noji S, Takahata E, Yaguchi T, Tsukamoto N, Kudo-Saito C, Hayashi Y, Kamiyama I, Ohtsuka T, Asamura H and Kawakami Y. Prognostic value of tumor-infiltrating lymphocytes differs depending on histological type and smoking habit in completely resected non-small-cell lung cancer. Ann Oncol 2016; 27: 2117-2123.
[23] Al-Shibli KI, Donnem T, Al-Saad S, Persson M, Bremnes RM and Busund LT. Prognostic effect of epithelial and stromal lymphocyte infiltration in non-small cell lung cancer. Clin Cancer Res 2008; 14: 5220-5227.
[24] Hernandez-Prieto S, Romera A, Ferrer M, Subiza JL, Lopez-Asenjo JA, Jarabo JR, Gomez AM, Molina EM, Puente J, Gonzalez-Larriba JL, Hernando F, Perez-Villamil B, Diaz-Rubio E and Sanz-Ortega J. A 50-gene signature is a novel scoring system for tumor-infiltrating immune cells with strong correlation with clinical outcome of stage I/II non-small cell lung cancer. Clin Transl Oncol 2015; 17: 330-338.
[25] Faruki H, Mayhew GM, Serody JS, Hayes DN, Perou CM and Lai-Goldman M. Lung adenocarcinoma and squamous cell carcinoma gene expression subtypes demonstrate significant

differences in tumor immune landscape. J Thorac Oncol 2017; 12: 943-953.
[26] Gentles AJ, Newman AM, Liu CL, Bratman SV, Feng W, Kim D, Nair VS, Xu Y, Khuong A, Hoang CD, Diehn M, West RB, Plevritis SK and Alizadeh AA. The prognostic landscape of genes and infiltrating immune cells across human cancers. Nat Med 2015; 21: 938-945.
[27] Hald SM, Bremnes RM, Al-Shibli K, Al-Saad S, Andersen S, Stenvold H, Busund LT and Donnem T. CD4/CD8 co-expression shows independent prognostic impact in resected non-small cell lung cancer patients treated with adjuvant radiotherapy. Lung Cancer 2013; 80: 209-215.
[28] Suzuki K, Kadota K, Sima CS, Nitadori J, Rusch VW, Travis WD, Sadelain M and Adusumilli PS. Clinical impact of immune microenvironment in stage I lung adenocarcinoma: tumor interleukin-12 receptor beta2 (IL-12Rbeta2), IL-7R, and stromal FoxP3/CD3 ratio are independent predictors of recurrence. J Clin Oncol 2013; 31: 490-498.
[29] Kurebayashi Y, Emoto K, Hayashi Y, Kamiyama I, Ohtsuka T, Asamura H and Sakamoto M. Comprehensive immune profiling of lung adenocarcinomas reveals four immunosubtypes with plasma cell subtype a negative indicator. Cancer Immunol Res 2016; 4: 234-247.
[30] Goc J, Germain C, Vo-Bourgais TK, Lupo A, Klein C, Knockaert S, de Chaisemartin L, Ouakrim H, Becht E, Alifano M, Validire P, Remark R, Hammond SA, Cremer I, Damotte D, Fridman WH, Sautes-Fridman C and Dieu-Nosjean MC. Dendritic cells in tumor-associated tertiary lymphoid structures signal a Th1 cytotoxic immune contexture and license the positive prognostic value of infiltrating CD8+ T cells. Cancer Res 2014; 74: 705-715.
[31] Dieu-Nosjean MC, Goc J, Giraldo NA, Sautes-Fridman C and Fridman WH. Tertiary lymphoid structures in cancer and beyond. Trends Immunol 2014; 35: 571-580.
[32] Coffelt SB, Wellenstein MD and de Visser KE. Neutrophils in cancer: neutral no more. Nat Rev Cancer 2016; 16: 431-446.
[33] Shaul ME and Fridlender ZG. Tumour-associated neutrophils in patients with cancer. Nat Rev Clin Oncol 2019; 16: 601-620.
[34] Rakaee M, Busund LT, Paulsen EE, Richardsen E, Al-Saad S, Andersen S, Donnem T, Bremnes RM and Kilvaer TK. Prognostic effect of intratumoral neutrophils across histological subtypes of non-small cell lung cancer. Oncotarget 2016; 7: 72184-72196.
[35] Liu X, Wu S, Yang Y, Zhao M, Zhu G and Hou Z. The prognostic landscape of tumor-infiltrating immune cell and immunomodulators in lung cancer. Biomed Pharmacother 2017; 95: 55-61.
[36] Carus A, Ladekarl M, Hager H, Pilegaard H, Nielsen PS and Donskov F. Tumor-associated neutrophils and macrophages in non-small cell lung cancer: no immediate impact on patient outcome. Lung Cancer 2013; 81: 130-137.
[37] Liu L, Ge D, Ma L, Mei J, Liu S, Zhang Q, Ren F, Liao H, Pu Q, Wang T and You Z. Interleukin-17 and prostaglandin E2 are involved in formation of an M2 macrophage-dominant microenvironment in lung cancer. J Thorac Oncol 2012; 7: 1091-1100.
[38] Sedighzadeh SS, Khoshbin AP, Razi S, Keshavarz-Fathi M and Rezaei N. A narrative review of tumor-associated macrophages in lung cancer: regulation of macrophage polarization and therapeutic implications. Transl Lung Cancer Res 2021; 10: 1889-1916.
[39] Welsh TJ, Green RH, Richardson D, Waller DA, O'Byrne KJ and Bradding P. Macrophage and mast-cell invasion of tumor cell islets confers a marked survival advantage in non-small-cell lung cancer. J Clin Oncol 2005; 23: 8959-8967.
[40] Ohtaki Y, Ishii G, Nagai K, Ashimine S, Kuwata T, Hishida T, Nishimura M, Yoshida J, Takeyoshi I and Ochiai A. Stromal macrophage expressing CD204 is associated with tumor aggressiveness in lung adenocarcinoma. J Thorac Oncol 2010; 5: 1507-1515.
[41] Rakaee M, Busund LR, Jamaly S, Paulsen EE, Richardsen E, Andersen S, Al-Saad S, Bremnes RM, Donnem T and Kilvaer TK. Prognostic value of macrophage phenotypes in resectable non-small cell lung cancer assessed by multiplex immunohistochemistry. Neoplasia 2019; 21: 282-293.
[42] Kawai O, Ishii G, Kubota K, Murata Y, Naito Y, Mizuno T, Aokage K, Saijo N, Nishiwaki Y, Gemma A, Kudoh S and Ochiai A. Predominant infiltration of macrophages and $CD8^+$ T cells in cancer nests is a significant predictor of survival in stage IV nonsmall cell lung cancer. Cancer 2008; 113: 1387-1395.
[43] Kinoshita F, Takada K, Yamada Y, Oku Y, Kosai K, Ono Y, Tanaka K, Wakasu S, Oba T, Osoegawa A, Tagawa T, Shimokawa M, Oda Y and Mori M. Combined evaluation of tumor-infiltrating CD8+ and FoxP3+ lymphocytes provides accurate prognosis in stage IA lung adenocarcinoma. Ann Surg Oncol 2020; 27: 2102-2109.
[44] Handa Y, Tsutani Y, Shiroma N, Kai Y, Mimae T, Miyata Y, Takeshima Y, Arihiro K and Okada M. Prognostic impact of programmed death-ligand 1 and surrounding immune status on stage I lung cancer. Clin Lung Cancer 2020; 21: e302-e314.